



# Temperature dependent current-voltage characteristics of Au/*n*-Si Schottky barrier diodes and the effect of transition metal oxides as an interface layer



Somnath Mahato<sup>a,b,\*</sup>, Joaquim Puigdollers<sup>b</sup>

<sup>a</sup> Saha Institute of Nuclear Physics (Surface Physics and Material Science), 1/AF Bidhannagar, Kolkata 700064, India

<sup>b</sup> Department of Electronic Engineering, Universitat Politècnica de Catalunya, Jordi Girona 1-3, Barcelona 08034, Spain

## ARTICLE INFO

### Keywords:

Schottky junctions  
TMO interface layer  
*I*-*V*-*T* measurements

## ABSTRACT

Temperature dependent current–voltage (*I*–*V*) characteristics of Au/*n*-type silicon (*n*-Si) Schottky barrier diodes have been investigated. Three transition metal oxides (TMO) are used as an interface layer between gold and silicon. The basic Schottky diode parameters such as ideality factor (*n*), barrier height ( $\phi_{b0}$ ) and series resistance (*R<sub>s</sub>*) are calculated and successfully explained by the thermionic emission (TE) theory. It has been found that ideality factor decreased and barrier height increased with increased of temperature. The conventional Richardson plot of  $\ln(I_0/T^2)$  vs.  $1000/T$  is determined the activation energy (*E<sub>a</sub>*) and Richardson constant (*A*<sup>\*</sup>). Whereas value of '*A*<sup>\*</sup>' is much smaller than the known theoretical value of *n*-type Si. The temperature dependent *I*–*V* characteristics obtained the mean value of barrier height ( $\overline{\phi_{b0}}$ ) and standard deviation ( $\sigma_s$ ) from the linear plot of  $\phi_{ap}$  vs.  $1000/T$ . From the modified Richardson plot of  $\ln(I_0/T^2) \rightarrow (q\sigma)^2/2(kT)^2$  vs.  $1000/T$  gives Richardson constant and homogeneous barrier height of Schottky diodes. Main observation in this present work is the barrier height and ideality factor shows a considerable change but the series resistance value exhibits negligible change due to TMO as an interface layer.

## 1. Introduction

Recent interests in transition metal oxides are stemmed predominantly from their reported high work function, semiconducting properties and good transparency. In particular, molybdenum trioxide (MoO<sub>3</sub>), vanadium pentoxide (V<sub>2</sub>O<sub>5</sub>) and tungsten trioxide (WO<sub>3</sub>) are used as for stacked in organic light emitting diodes (OLED) [1], buffer layer for photovoltaic devices [2,3], interface layer for Schottky barrier diodes [4] and other solid-state electronic devices [5] etc. Schottky barrier diodes (SBDs) are consist of a metal–semiconductor (MS) junction whose properties depend on the work function, bandgap, dopants concentration and the interface layer between metal and semiconductor. The control of this interface property has great importance in many electronics device applications [6,7]. The effect of the interface layer on SBDs can be easily modified by using suitable organic materials, polymers or metal oxides. Taşcıoğlu et al. [8], reported that the MS structures with organic interface layer which plays an important role in the semiconductor device application. Whereas Tunc et al., [9] used PVA film (doped with different ratios of nickel (Ni) and zinc (Zn)) as an interface layer between gold and *n*-type Silicon. Meanwhile, Yuksel et al., [10] used spin coated perylene-monoimide (PMI) organic semiconductor on *n*-Si wafer and

formed a Schottky barrier junction. Finally, Chen et al., [11] reported the presence of a thin interface layer of Molybdenum oxide between the metal and semiconductor referred to as metal/oxide/semiconductors (MOS) Schottky barrier diodes. This MOS device has become more popular compared with the other types of SBDs because of their many device applications [12,13].

Recently the binary TMO, such as MoO<sub>3</sub>, V<sub>2</sub>O<sub>5</sub> and WO<sub>3</sub> are used as a hole-injecting buffer layers for alternative hole selective emitters in heterojunction solar cells [14]. The charge transport phenomenon at room temperature *I*–*V* measurement was not enough to know the details about electrical property across the MS junction. Therefore, taking the temperature dependent *I*–*V* measurement is necessary to get sufficient information about electrical parameters of the Au/*n*-Si junction. In this present report, we demonstrated the effect of TMO as an interface layer on Au/*n*-Si Schottky junction. Barrier height, ideality factor, series resistance, activation energy and Richardson constant are calculated for Au/*n*-Si and compared with Au/TMO/*n*-Si Schottky junction.

## 2. Experimental section

Double side polished *n*-type float zone c-Si (100) wafers were used as

\* Saha Institute of Nuclear Physics (Surface Physics and Material Science), 1/AF Bidhannagar, Kolkata 700064, India.

E-mail address: [som.phy.ism@gmail.com](mailto:som.phy.ism@gmail.com) (S. Mahato).

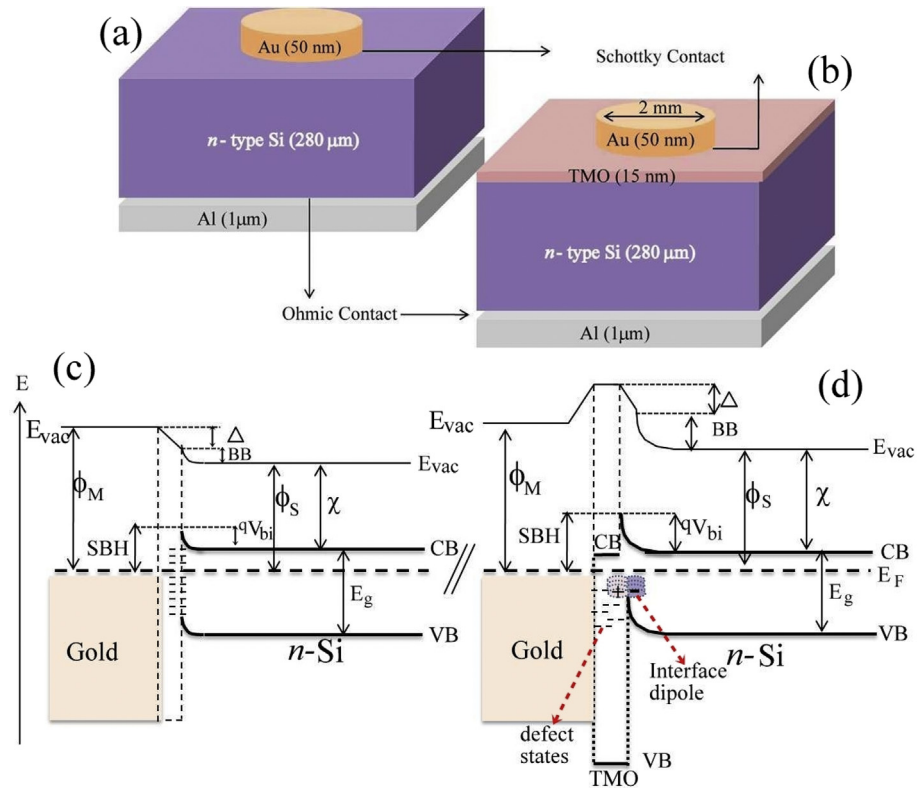


Fig. 1. [(a) & (b)] Schematic diagrams and [(c) & (d)] band diagram of Au/*n*-Si and Au/TMO/*n*-Si Schottky barrier diodes (SBDs) where as SBH is Schottky barrier height, BB is band bending,  $\phi_M$  &  $\phi_S$  is the work function of metal and semiconductor  $\chi$  is the electron affinity and  $\Delta$  is the interface dipole.

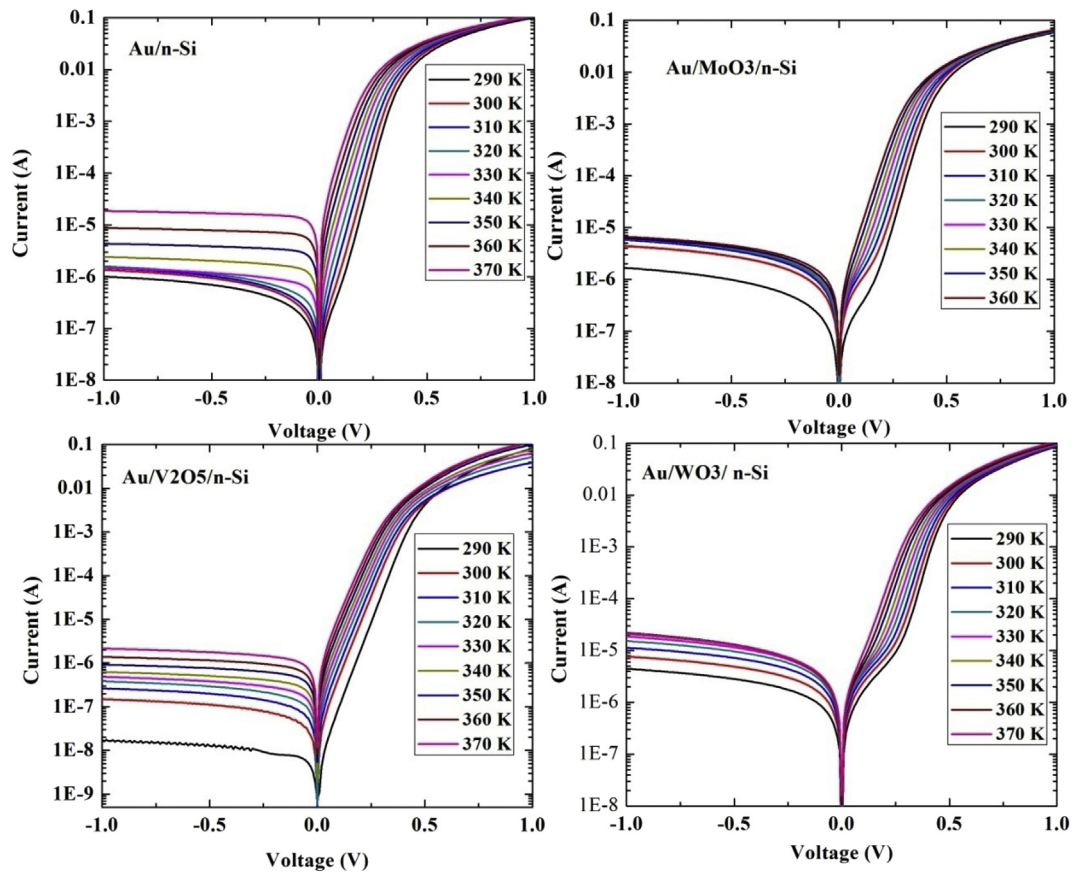


Fig. 2. Forward and reverse bias semi-logarithmic current–voltage (*I*–*V*) characteristics of Au/*n*-Si and Au/TMO/*n*-Si SBDs in the temperature range 290 K–370 K.

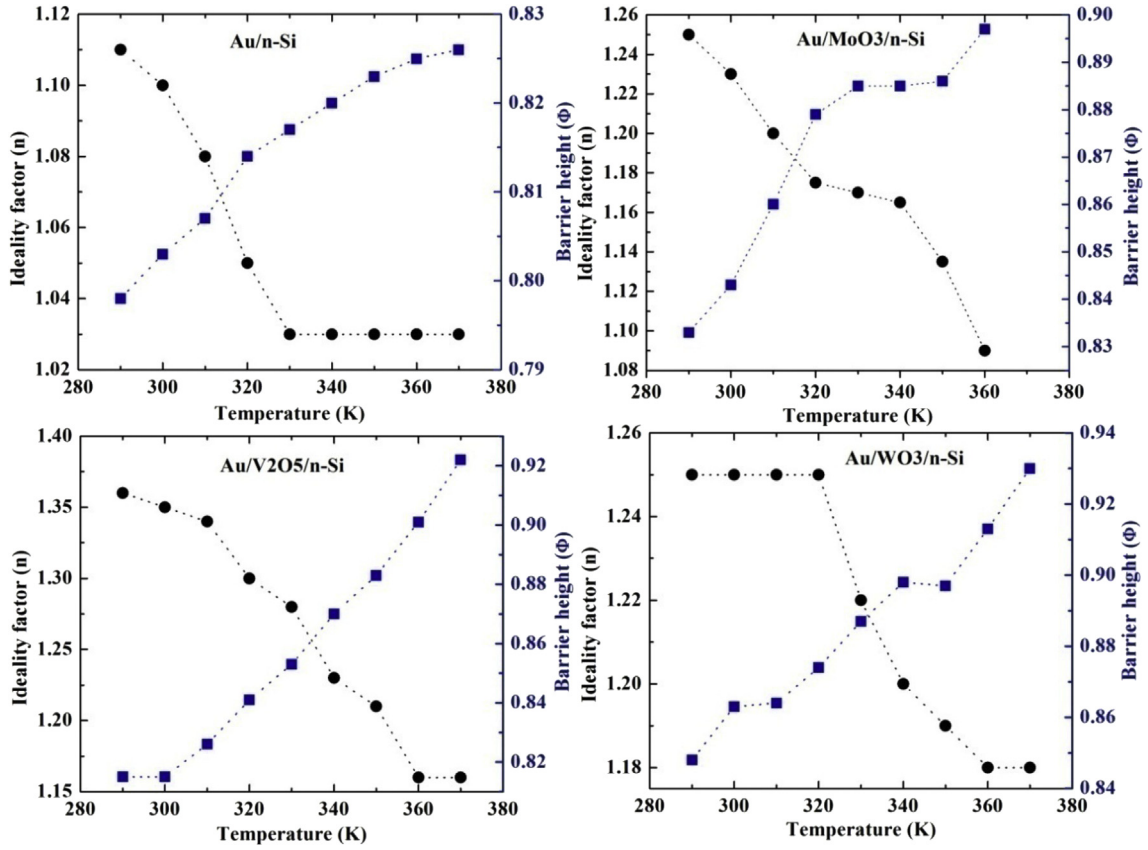


Fig. 3. Temperature dependence of the ideality factor ( $n$ ) and the barrier height ( $\phi_{b0}$ ) of Au/ $n$ -Si and Au/TMO/ $n$ -Si SBDs.

substrates. Resistivity and thickness of the wafer was 2.5  $\Omega$ -cm and 280  $\mu$ m respectively. The wafers were cleaned by standard RCA cleaning and dipped in 1% HF acid during 1 min for native oxide removal. The Au/ $n$ -Si Schottky contact was made onto the  $n$ -Si wafer with high purity gold deposited by thermal evaporation process through a shadow mask. The thickness of the gold was 50 nm. For Au/TMO/ $n$ -Si SBDs, a thin layer (15 nm) of three consecutive transition metal oxides (Sigma Aldrich, 99.9%) were deposited by thermal evaporation (pressure  $10^{-6}$  mbar) process at the deposition rate 0.2  $\text{\AA}/\text{s}$  before gold deposition. Finally, more than 1  $\mu$ m thick Aluminum was thermally evaporated as a back ohmic contact. The schematic diagram of Au/ $n$ -Si and Au/TMO/ $n$ -Si Schottky barrier diodes are shown in Fig. 1[(a) & (b)]. The current-voltage ( $I$ - $V$ ) measurements were performed by a Keithley 2400 source meter at a temperature range between 290 K and 370 K using temperature controller.

### 3. Results and discussion

The most useful method to characterize the electrical parameters of a metal semiconductor junction is based on temperature dependent current-voltage measurement. The thermionic  $I$ - $V$  characteristics of SBDs at forward and reverse bias (neglecting series and shunt resistance), is expressed by Ref. [15].

$$I = I_0 \left[ \exp\left(\frac{qV}{nkT}\right) - 1 \right] \quad (1)$$

where  $I_0$  is the reverse saturation current derived from the straight line fitting at intercept of current axis is given by

$$I_0 = AA^*T^2 \exp\left(\frac{-q\phi_{b0}}{kT}\right) \quad (2)$$

where  $A$  is the area of diode,  $\phi_{b0}$  is the barrier height,  $q$  is the electron charge,  $k$  is the Boltzmann constant.  $T$  is the absolute temperature,  $A^* = \frac{4\pi qm^*k^2}{h^3}$  is Richardson's constant and the value is  $120 \text{ A}\cdot\text{cm}^{-2}\cdot\text{K}^{-2}$  for  $n$ -type Si [9,16]. The ideality factor and barrier height of the SBDs are describe the deviation of the experimental temperature dependent  $I$ - $V$  data is expressed as:

$$n = \frac{q}{kT} \frac{dV}{d\ln I} \quad (3)$$

$$\phi_{b0} = \frac{kT}{q} \ln\left(\frac{AA^*T^2}{I_0}\right) \quad (4)$$

Fig. 2 shown the semi-logarithmic forward and reverse bias  $I$ - $V$  characteristics of the Au/ $n$ -Si and Au/TMO/ $n$ -Si SBDs in the different temperature range. From intercepts and slopes of  $\ln I$  vs.  $V$  plot at each temperature gives the  $\phi_{b0}$  and  $n$  respectively. The range of  $\phi_{b0}$  and  $n$  for the Au/ $n$ -Si SBDs are from 0.79 eV to 1.11 at 290 K to 0.82 eV and 1.03 at 370 K. The experimental value of  $n$  (indicated by circles) and  $\phi_{b0}$  (indicated by squares) obtained depending on the temperature. Calculated  $\phi_{b0}$  value increased and  $n$  decreased with the increasing temperature (shown in Fig. 3) due to an inhomogeneity occurs in between MS interface which becomes more pronounced with the increases of temperature [8,17]. It is also found that the barrier height of Au/TMO/ $n$ -Si Schottky diode is higher than that of Au/ $n$ -Si Schottky diode. This suggests that the use of TMO as an interface layer modifies the effective barrier height by influencing the space charge region of the Au/ $n$ -Si Schottky junction as well as the increased the lateral inhomogeneity at the interface between gold and silicon. Therefore, the used of TMO plays an important role to produces a substantial shift in the work function of the gold and in the electron affinity of silicon. Finally, an excess barrier height is found due to TMO interface layer. The near unity ideality factor of the Au/ $n$ -Si Schottky

**Table 1**

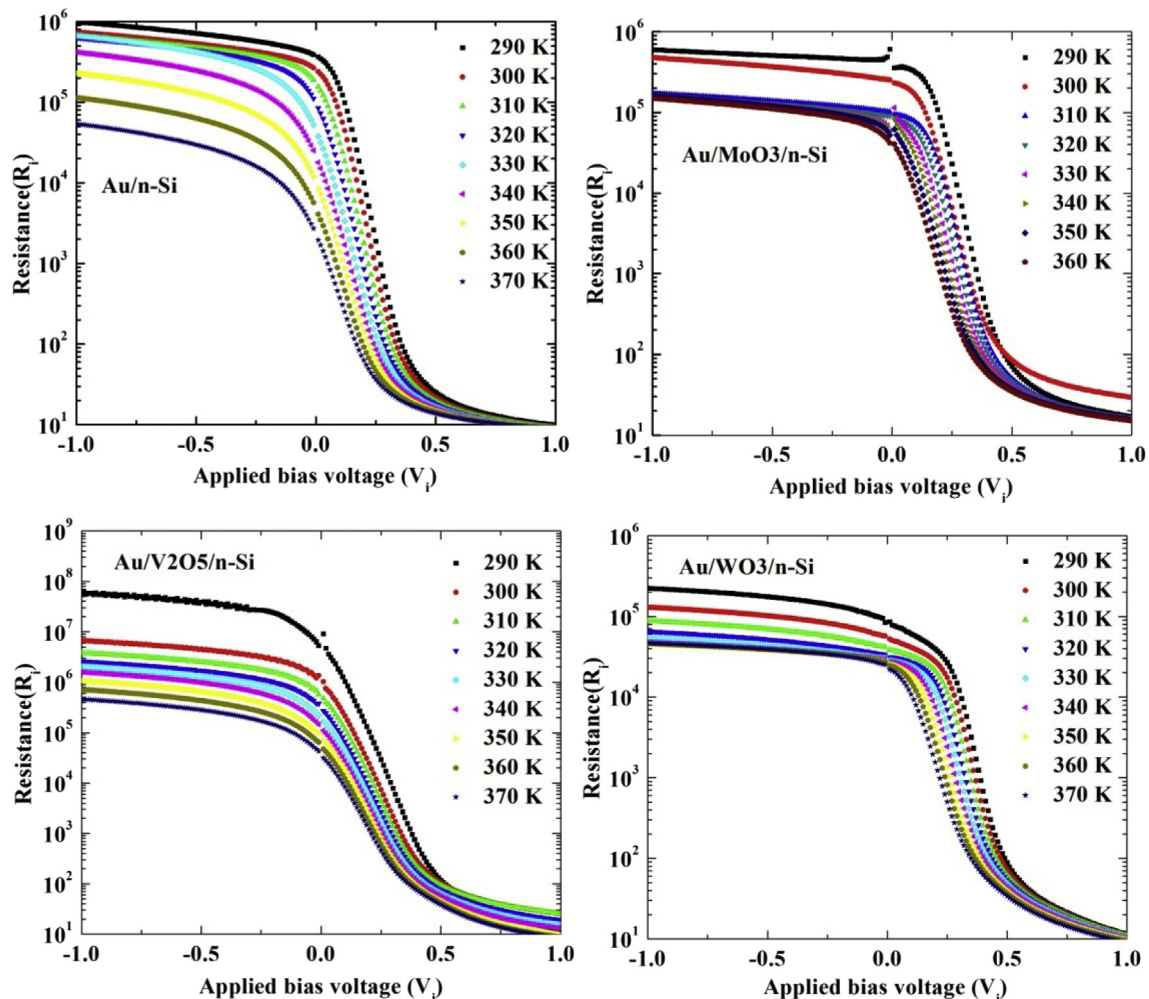
Temperature dependent electrical parameters of the Au/n-Si and Au/TMO/n-Si SBDs determined from I–V–T measurements.

T(K)	Au/n-Si			Au/MoO <sub>3</sub> /n-Si			Au/V <sub>2</sub> O <sub>5</sub> /n-Si			Au/WO <sub>3</sub> /n-Si		
	$\phi_{b0}$ [eV]	$n$	$R_s$ [ $\Omega$ ]	$\phi_{b0}$ [eV]	$n$	$R_s$ [ $\Omega$ ]	$\phi_{b0}$ [eV]	$n$	$R_s$ [ $\Omega$ ]	$\phi_{b0}$ [eV]	$n$	$R_s$ [ $\Omega$ ]
290	0.798	1.11	3.738	0.833	1.25	4.901	0.815	1.36	3.715	0.848	1.25	3.744
300	0.803	1.10	3.673	0.843	1.23	4.742	0.815	1.35	6.131	0.863	1.25	3.715
310	0.807	1.08	3.688	0.860	1.20	4.844	0.826	1.34	6.143	0.864	1.25	3.691
320	0.814	1.05	3.695	0.879	1.17	4.866	0.841	1.3	5.058	0.874	1.25	3.704
330	0.817	1.03	3.742	0.885	1.17	4.879	0.853	1.28	4.501	0.887	1.22	3.684
340	0.82	1.03	3.774	0.885	1.16	4.915	0.87	1.23	4.126	0.898	1.20	3.652
350	0.823	1.03	3.826	0.886	1.13	4.937	0.883	1.21	3.583	0.897	1.19	3.639
360	0.825	1.03	3.856	0.897	1.09	4.966	0.901	1.16	3.367	0.913	1.18	3.598
370	0.826	1.03	3.897	–	–	–	0.922	1.16	3.361	0.930	1.18	3.515

diode indicates that the diffusion of charge carrier across the interface of Schottky contact could be a main contributor to the current flow through metal-semiconductor junction. But the presence of TMO as an interface layer on Au/n-Si Schottky contact exhibited to increase ideality factor as well as barrier height. This could be attributed to interface dipoles formed by TMO and the high band bending at MS junction [17–19]. Fig. 1[(c) & (d)] shows the band structure of Au/n-Si and Au/TMO/n-Si SBDs. The calculated barrier height and ideality factor at each temperature of Au/n-Si and Au/TMO/n-Si SBDs are shown in Table 1.

In MS contacts, the series resistance ( $R_s$ ) and shunt resistance ( $R_{sh}$ ) are the important parameters governing the electrical property of Schottky barrier junction. Both the  $R_s$  and  $R_{sh}$  values are important which considerably influence the performance of the many electronic device

application especially on solar cell. In an ideal solar cell, the value  $R_s$  is as much as possible as low (m  $\Omega$  to  $\Omega$ ) whereas  $R_{sh}$  is as much as possible as high (in the order of K $\Omega$  to M $\Omega$ ). Therefore, here the experimental  $R_s$  and  $R_{sh}$  values are determined by plotting structure resistance ( $R_i$ ) vs. applied bias voltage ( $V_i$ ) shown in Fig. 4. It has been observed that at high forward bias voltage, the value of  $R_i$  becomes constant for all temperature, which corresponds to  $R_s$ . Subsequently, at negative bias voltage, the value of  $R_i$  becomes constant for all temperature which corresponds to  $R_{sh}$ . Thus, the values of series resistance of Au/n-Si SBDs are varied from 8  $\Omega$  to 10  $\Omega$  at 290 K–370 K. But the use of TMO as an interface layer this  $R_s$  value varies from 8  $\Omega$  to 30  $\Omega$  in the same temperature range. The low value of  $R_s$  can be attributed to the formation of interface dipole between metal and semiconductor or by the transportation of charge carrier

**Fig. 4.** The diode resistance ( $R_i$ ) vs.  $V_i$  plot of Au/n-Si and Au/TMO/n-Si SBDs for various temperatures.



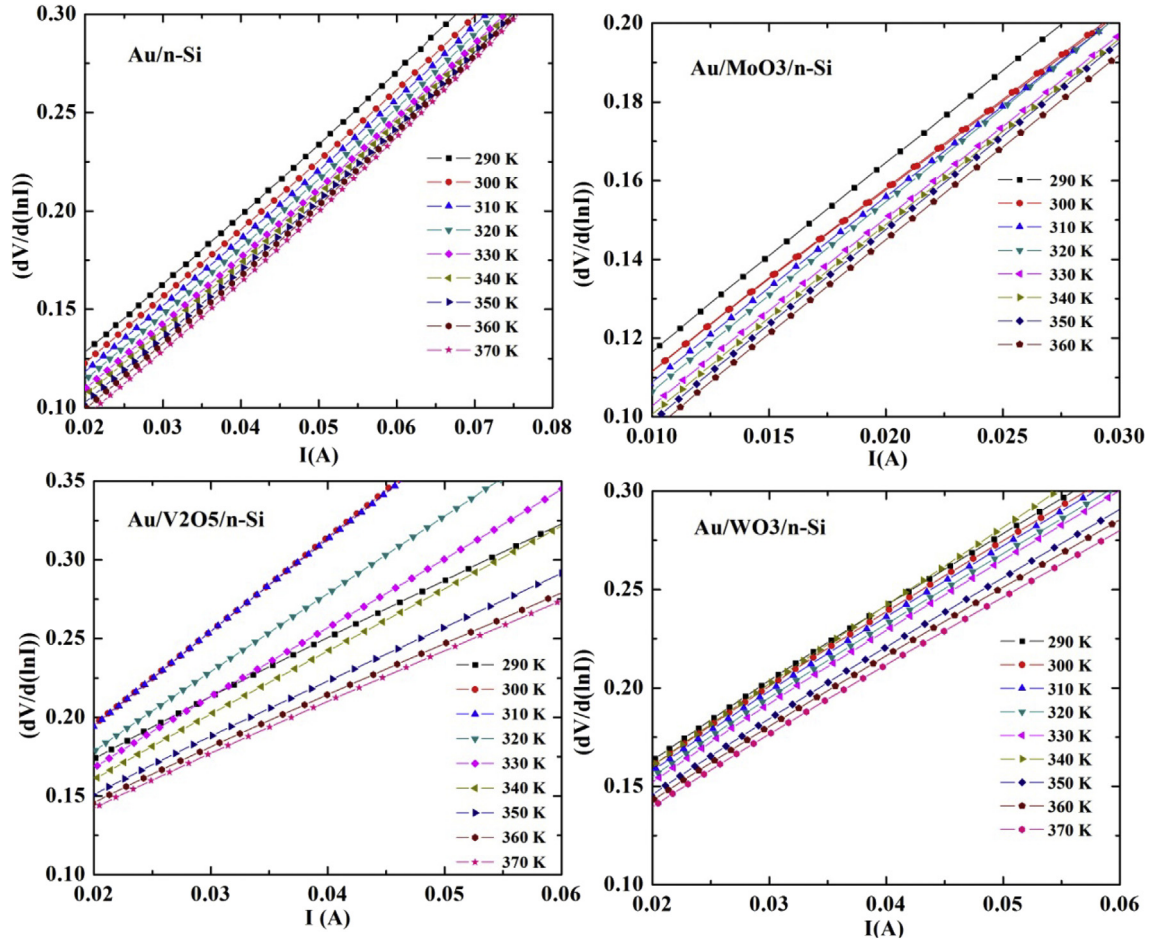


Fig. 5. Temperature dependence plot of  $dV/d(\ln I)$  vs.  $I$  for Au/n-Si and Au/TMO/n-Si SBDs.

through inversion layer or enhanced tunnelling current through the BH by using heavily doped  $n$ -type Si. On the other hand, we also evaluated the  $R_{sh}$  can be originated from leakage current and an interface paths along the layer between the front and back junction. The values of  $R_{sh}$  are found to be the order of  $10^4 \Omega$ – $10^8 \Omega$  for Au/n-Si and Au/TMO/n-Si SBDs.

In order to accurately determine the series resistances by Cheung and Cheung equation [20] using the forward bias  $I$ – $V$  relation due to thermionic emission of a Schottky contact is defined as:

$$\frac{dV}{d(\ln I)} = IR_s + \frac{nkT}{q} \quad (5)$$

The experimental series resistance value of Schottky diodes with and without interface layer are calculated from  $dV/d(\ln I)$  vs.  $I$  plot according to Eq. (6). The plot of  $dV/d(\ln I)$  vs.  $I$  give a straight line shown in Fig. 5. The value of  $R_s$  obtained from the slope of the graph. Corresponding calculated values are shown in Table 1. It should be noted that the series resistance of Au/TMO/n-Si Schottky junction is small change compared to the Au/n-Si Schottky junction. This implies that the effect of TMO on series resistance is ineffective at Au/n-Si Schottky junction. As a conclusion, all these three TMO can be suitable materials for solar cell application.

In order to find out the voltage dependent barrier height in forward bias  $I$ – $V$  region is to make use of conventional activation energy plot of the reverse saturation current  $I_0$ . Therefore, Eq. (2) can be rewritten as [21]:

$$\ln\left(\frac{I_0}{T^2}\right) = \ln(AA^*) - \frac{q\phi_{b0}}{kT} \quad (6)$$

A conventional activation energy or Richardson plot of  $\ln(I_0/T^2)$  vs.  $1000/T$  is shown in Fig. 6. As can be seen in Fig. 6, the Richardson plot is found to be linear in the temperature range from 290 K to 370 K. From the best fit of the linear region, activation energy ( $E_a$ ) and Richardson constant ( $A^*$ ) are calculated corresponding to each voltage. The value of  $E_a$  is obtained from the slope of straight lines as 0.69 eV for the Au/n-Si device, which is found to be higher than the half of the band gap of silicon ( $E_g/2$ ). The Richardson constant value of  $A^* = 1.06 \times 10^{-4} \text{ A}\cdot\text{cm}^{-2}\cdot\text{K}^{-2}$  is determined from the intercept at the experimental Richardson plot which is much smaller than the known theoretical value for  $n$ -type Si. To obtained above experimental results reveal that the variation in Richardson constant ( $A^*$ ) obtained from the Richardson plot may be affected by the lateral inhomogeneity of the Gaussian distribution of barrier height. Additionally the fact is that, it is different from the theoretical value may be connected to a value of the real effective mass that is different from the calculated one. In the above discussions, we can say that the predominant current conduction mechanism in Au/n-Si SBDs can be explained by the TE theory. From the similar plot between  $\ln I_0/T^2$  vs.  $1000/T$  we can calculate the activation energy and Richardson constant for Au/TMO/n-Si SBDs. The value of  $E_a$  is found to be lower than the half of the band gap of silicon ( $E_g/2$ ) for Au/V<sub>2</sub>O<sub>5</sub>/n-Si Schottky diodes. The overall Schottky contact is not uniform but consists of a series of low and high barrier patches, which is affected by interface TMO layers. Thus, due to the lateral inhomogeneity of the barrier height  $E_a$  and  $A^*$  values are obtained from the temperature dependent  $I$ – $V$  characteristics varies from diode to diode and shown in Table 2.

Some authors [22–24] treated a system of discrete interface regions or “patches” of barrier height to explain the observed barrier inhomogeneity from classical TE theory. The variation in BH may occur

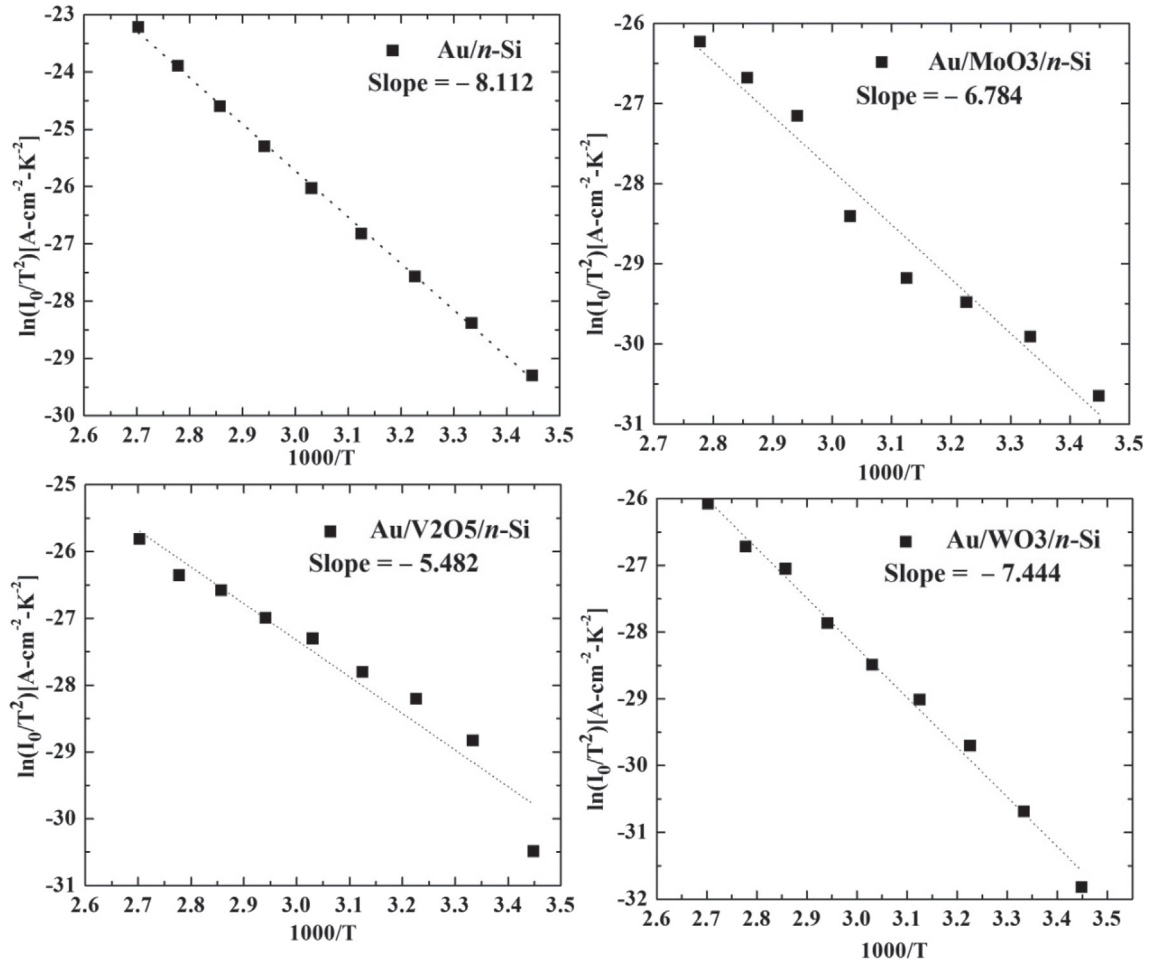


Fig. 6. Richardson plots of the  $\ln(I_0/T^2)$  vs.  $1000/T$  for Au/*n*-Si and Au/TMO/*n*-Si SBDs in the temperature range 290 K–370 K.

Table 2

Electronic parameters of Au/*n*-Si and Au/TMO/*n*-Si Schottky barrier diodes.

SBDs	Richardson plot	Modified Richardson plot						
	$E_a$ [eV]	$A^*$ [ $\text{Acm}^{-2}\text{K}^{-2}$ ]	$\overline{\phi_{b0}}$ [eV]	$\sigma_s$	$\rho_2$	$\rho_3$	$E_a$ [eV]	$A^*$ [ $\text{Acm}^{-2}\text{K}^{-2}$ ]
Au/ <i>n</i> -Si	0.69	$1.06 \times 10^{-4}$	0.93	0.082	0.377	0.138	0.93	138.41
Au/MoO <sub>3</sub> / <i>n</i> -Si	0.58	$4.50 \times 10^{-3}$	1.16	0.127	0.325	0.153	1.16	163.14
Au/V <sub>2</sub> O <sub>5</sub> / <i>n</i> -Si	0.47	$1.49 \times 10^{-4}$	1.30	0.158	0.373	0.190	1.36	1027.26
Au/WO <sub>3</sub> / <i>n</i> -Si	0.64	$7.99 \times 10^{-3}$	1.19	0.132	0.102	0.092	1.25	1069.16

even at a scale much smaller than the depletion region width ( $W_D$ ). In this case, the charge transport mechanism across the Schottky diodes may be significantly affected by the existence of the barrier inhomogeneity at the MS interface. Experimentally we plotted zero-bias barrier height  $\phi_{b0}$  vs. ideality factor  $n$  for Au/*n*-Si and Au/TMO/*n*-Si shown in Fig. 7. It is observed that zero-bias BH ( $\phi_{b0}$ ) increases with the decreases of ideality factor ( $n$ ), which is responsible for the lateral BH inhomogeneity presence at the interfaces in real SBDs. The extrapolation of  $\phi_{b0}$  vs.  $n$  plot to  $n = 1$  has given a homogeneous  $\phi_{b0}$  of approximately 0.82 eV for Au/*n*-Si diodes. The other corresponding  $\phi_{b0}$  values of Au/TMO/*n*-Si diodes are 0.94 eV, 0.97 eV and 0.99 eV for MoO<sub>3</sub>, V<sub>2</sub>O<sub>5</sub> and WO<sub>3</sub> interface layer respectively. The significant increase of the zero-bias  $\phi_{b0}$  and increase of  $n$  especially at high temperatures are possibly caused by the inhomogeneity increased at the metal-semiconductor interface.

The above abnormal behavior can be explained using an analytical potential fluctuation model based on inhomogeneous barrier heights at the interface between metal and semiconductor. Let us assume that the double Gaussian distribution of apparent BH ( $\phi_{ap}$ ) and the apparent

ideality factor ( $n_{ap}$ ), with a mean barrier height ( $\overline{\phi_{b0}}$ ) and standard deviations ( $\sigma_s$ ) can be expressed by the following relations [25]:

$$\phi_{ap} = \overline{\phi_{b0}}(T=0) - \frac{q\sigma_s^2}{2kT} \quad (7)$$

$$\left(\frac{1}{n_{ap}} - 1\right) = \rho_2 - \frac{q\rho_3}{2kT} \quad (8)$$

It is conceded that the mean BH,  $\overline{\phi_{b0}}$  and  $\sigma_s$  are linearly bias dependent on Gaussian parameters such as  $\phi_b = \overline{\phi_{b0}} + \rho_2 V$  and standard deviation,  $\sigma_s = \sigma_0 + \rho_3 V$  where  $\rho_2$  and  $\rho_3$  are voltage coefficients which may depend on temperature and quantify the voltage deformation of the barrier height distribution. Fitting of the experimental data into Eq. (7) and Eq. (8). Thus, we have attempted to draw a  $\phi_{ap}$  vs.  $1000/T$  plot (Fig. 8) to obtain the  $\overline{\phi_{b0}}$  and  $\sigma_s$  at zero bias of a double Gaussian distribution of the BH. Also, as it can be seen from Fig. 9, the plot of  $((1/n_{ap}) - 1)$  vs.  $1000/T$  gives a straight line and evaluate the value of  $\rho_2$  obtained

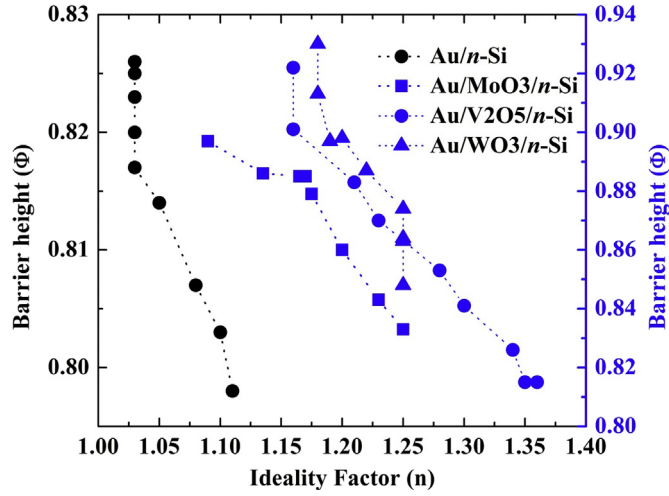


Fig. 7. Zero-bias barrier height vs. the ideality factor of Au/n-Si and Au/TMO/n-Si Schottky diode at different temperatures.

from the intercept and the value of  $\rho_3$  from the slope. These results indicate the presence of a double Gaussian distribution of BH in the Schottky contact area. Now, the conventional Richardson plot can be modified by combining with Eq. (2) and Eq. (7) as follows:

$$\ln\left(\frac{I_0}{T^2}\right) - \frac{q^2\sigma_0^2}{2k^2T^2} = \ln(AA^*) - q\frac{\bar{\phi}_{b0}}{kT} \quad (9)$$

Thus the plot of modified activation energy according to Eq. (9)

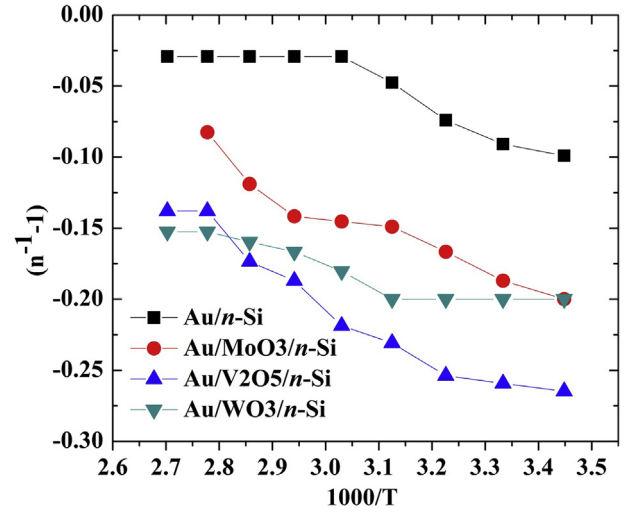


Fig. 9.  $((1/n_{ap}) - 1)$  vs.  $1000/T$  curves of Au/n-Si and Au/TMO/n-Si SBDs according to the double GD of BH.

should give a straight line. Slope, which directly yields the mean barrier height ( $\bar{\phi}_{b0}$ ) and intercepts ( $=\ln AA^*$ ) at ordinate determined  $A^*$  for a given diode area  $A$ . In Fig. 10, the modified  $\ln(I_0/T^2) - (q\sigma)^2/2(kT)^2$  vs.  $1000/T$  plot gives  $\bar{\phi}_{b0}$  ( $T = 0$ ) and  $A^*$  as 0.93 eV and  $138.41 \text{ A-cm}^{-2}\text{-K}^{-2}$  respectively for Au/n-Si SBDs. It is cleared that the value of  $\bar{\phi}_{b0} = 0.93 \text{ eV}$  obtained from the modified activation energy plot is approximately same as the value of  $\bar{\phi}_{b0} = 0.93 \text{ eV}$  from  $\phi_{ap}$  vs.  $1000/T$  plot. Simultaneously we extracted  $\bar{\phi}_{b0}$  and  $A^*$  values for Au/TMO/n-Si SBDs are shown in Table 2.

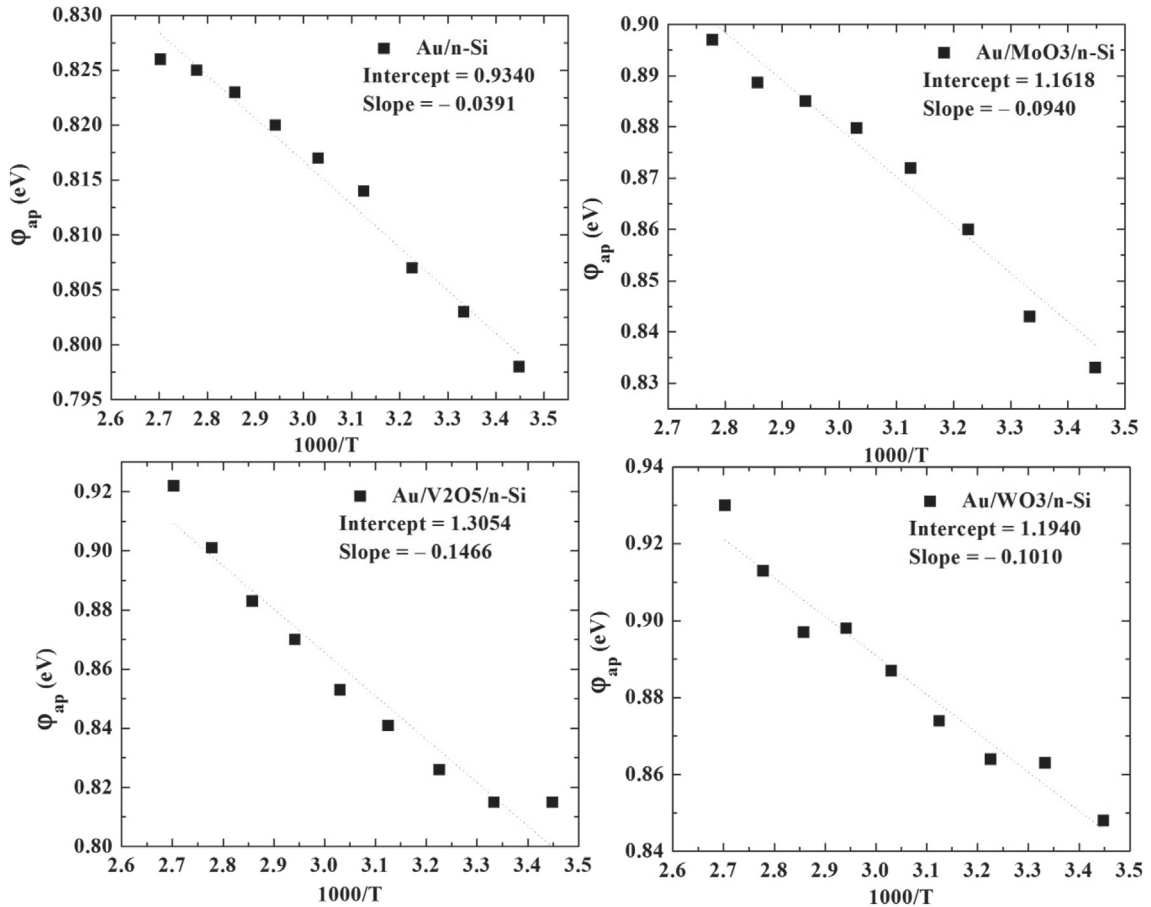


Fig. 8.  $\phi_{ap}$   $1000/T$  curves of Au/n-Si and Au/TMO/n-Si SBDs according to the double GD of BH.

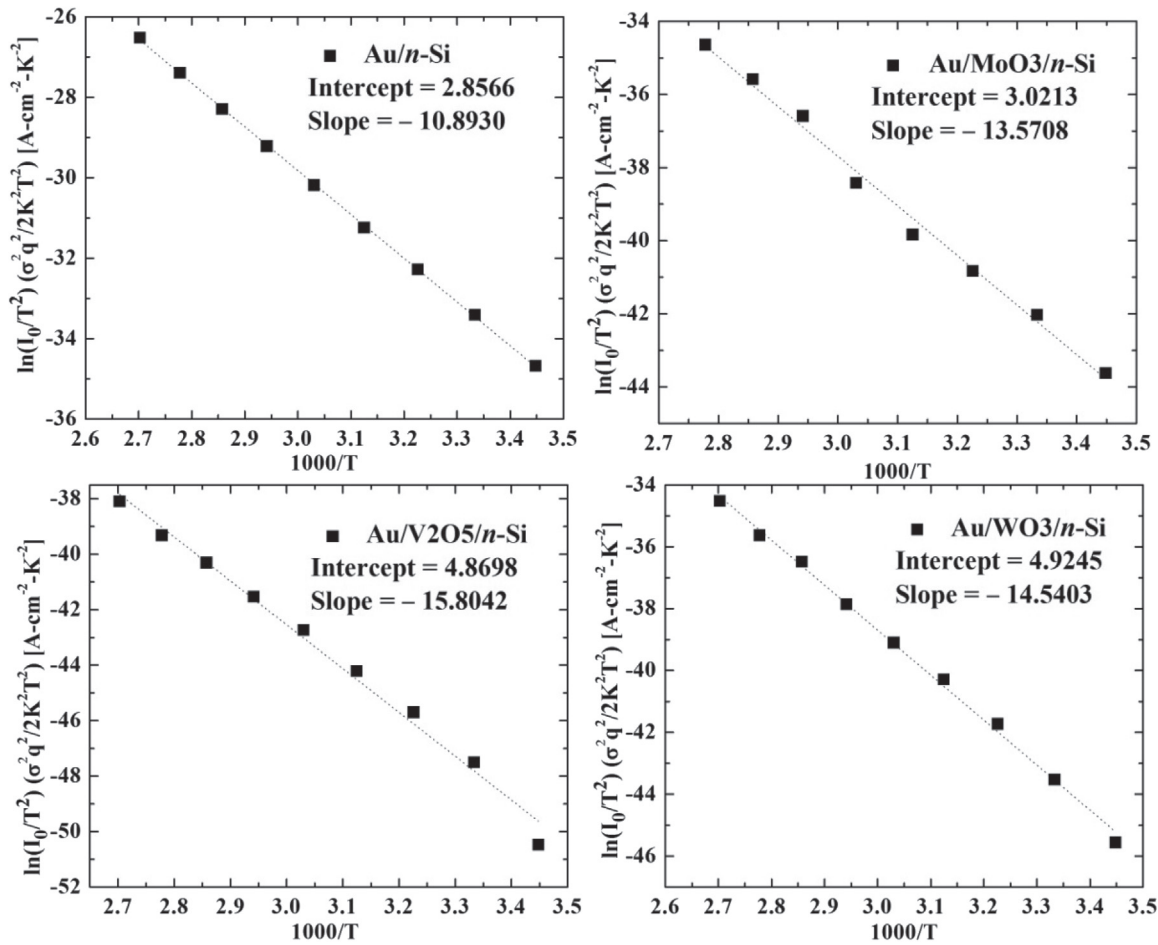


Fig. 10. Modified Richardson  $\ln(I_0/T^2) \rightarrow (q\sigma)^2/2(kT)^2$  vs.  $1000/T$  plot for Au/n-Si and Au/TMO/n-Si SBDs according to the double GD of BH.

It can be seen, the value of  $\overline{\phi_{b0}}$  from modified activation energy plot is closed with the value of  $\overline{\phi_{b0}}$  from the plot of  $\phi_{ap}$  vs.  $1000/T$ . However the  $A^*$  value is large for Au/V<sub>2</sub>O<sub>5</sub>/n-Si and Au/WO<sub>3</sub>/n-Si SBDs compare to the known theoretical value of  $120 \text{ A}\cdot\text{cm}^{-2}\cdot\text{K}^{-2}$  for *n*-type Si.

#### 4. Conclusions

The current conduction across the MS and MOS junction of Au/n-Si and Au/TMO/n-Si SBDs have been investigated by using forward and reversed bias current–voltage characteristics in the temperature ranging from 290 K to 370 K. The obtained barrier height and ideality factor of Au/n-Si and Au/TMO/n-Si Schottky junctions are found to be a function of temperature. Evaluating the experimental  $I$ – $V$ – $T$  data reveals an abnormal increase in  $\phi_{b0}$  and decrease in  $n$  with increasing temperature that attributed to the barrier inhomogeneity. The values of  $R_s$  are determined from Cheung's function and the observed  $R_s$  values exhibit an invariable behavior with the use of TMO as an interface layer. Modified Richardson plot  $\ln(I_0/T^2) - (q\sigma)^2/2(kT)^2$  vs.  $1000/T$  gives the closer value of Richardson constant for Au/n-Si SBDs. We believed that transition metal oxides have the particular advantages as an interface layer in Au/n-Si Schottky junction due to its good rectifying property, increase barrier height, ideality factor close to one and low series resistance.

#### Acknowledgements

This work is supported by Erasmus Mundus Action 2 AREAS+ grant programs. Authors are thankful to Mr. Luis G. Gerling of Department of Electronic Engineering, Universitat Politècnica de Catalunya, Barcelona, Spain for his supports.

#### References

- [1] S. Hamwi, J. Meyer, M. Kroger, T. Winkler, M. Witte, T. Riedl, A. Kahn, W. Kowalsky, The role of transition metal oxides in charge- generation layers for stacked organic light-emitting diodes, *Adv. Funct. Mater.* 20 (2010) 1762–1766.
- [2] W. Wu, J. Bao, X. Jia, Z. Liu, L. Cai, B. Liu, J. Song, H. Shen, Dopant-free back contact silicon heterojunction solar cells employing transition metal oxide emitters, *Phys. Status Solidi RRL* (2016) 1–6.
- [3] J. Geissbuhler, J. Werner, S.M. de Nicolas, L. Barraud, A.H. Wyser, M. Despeisse, S. Nicolay, A. Tomasi, B. Niesen, S. De Wolf, C. Ballif, 22.5% efficient silicon heterojunction solar cell with molybdenum oxide hole collector, *Appl. Phys. Lett.* 107 (2015), 081601.
- [4] B. Kinaci, S.S. Cetin, A. Bengi, S. özcelik, The temperature dependent analysis of Au/TiO<sub>2</sub> (rutile)/n-Si (MIS) SBDs using current–voltage–temperature ( $I$ – $V$ – $T$ ) characteristics, *Mater. Sci. Semicond. Process.* 15 (2012) 531–535.
- [5] J. Meyer, S. Hamwi, M. Kröger, W. Kowalsky, T. Riedl, A. Kahn, Transition metal oxides for organic electronics: energetics, device physics and applications, *Adv. Mater.* (2012) 1–20.
- [6] J.Y. Park, H. Lee, J.R. Renzas, Y. Zhang, G.A. Somorjai, Probing hot electron flow generated on Pt nanoparticles with Au/TiO<sub>2</sub> Schottky diodes during catalytic CO oxidation, *Nano Lett.* 8 (2008) 2388–2392.
- [7] K.Y. Mitra, C. Sternkiker, C.M. Domingo, E. Sowade, E. Ramon, J. Carrabina, H.L. Gomes, R.R. Baumann, Inkjet printed metal insulator semiconductor (MIS) diodes for organic and flexible electronic application, *Flex. Print. Electron.* 2 (2017), 015003.
- [8] İ. Taşoğlu, U. Aydemir, S. Altındal, The explanation of barrier height inhomogeneities in Au/n-Si Schottky barrier diodes with organic thin interfacial layer, *J. Appl. Phys.* 108 (2010) 064506.
- [9] T. Tunc, S. Altındal, I. Uslu, I. Dökme, H. Uslu, Temperature dependent current–voltage( $I$ – $V$ ) characteristics of Au/n-Si (111) Schottky barrier diodes with PVA(Ni,Zn-doped) interfacial layer, *Mater. Sci. Semicond. Process.* 14 (2011) 139–145.
- [10] O.F. Yuksel, M. Kus, N. Simsir, H. Safak, M. Sahin, E. Yenal, A detailed analysis of current–voltage characteristics of Au/perylene-monoimide/n-Si Schottky barrier diodes over a wide temperature range, *J. Appl. Phys.* 110 (2011), 024507.
- [11] J. Chen, J. Lv, Q. Wang, Electronic properties of Al/MoO<sub>3</sub>/p-InP enhanced Schottky barrier contacts, *Thin Solid Films* 616 (2016) 145–150.



- [12] S.H.S. Chan, T.Y. Wu, J.C. Juan, C.Y. Teha, Recent developments of metal oxide semiconductors as photocatalysts in advanced oxidation processes (AOPs) for treatment of dye waste–water, *J. Chem. Technol. Biotechnol.* 86 (2011) 1130–1158.
- [13] F. Yakuphanoglu, B.F. Şenkal, Electronic and thermoelectric properties of polyaniline organic semiconductor and electrical characterization of Al/PANI MIS diode, *J. Phys. Chem. C* 111 (2007) 1840–1846.
- [14] L.G. Gerling, S. Mahato, A.M. Vilches, G. Masmitja, P. Ortega, C. Voz, R. Alcubilla, J. Puigdollers, Transition metal oxides as hole-selective contacts in silicon heterojunctions solar cells, *Sol. Energy Mater. Sol. Cells* 145 (2016) 109–115.
- [15] Ş. Aydoğan, Ö. Güllü, A. Türit, Fabrication and electrical characterization of a silicon Schottky device based on organic material, *Phys. Scr.* 79 (2009), 035802.
- [16] M.A. Yeganeh, S.H. Rahmatollahpur, Barrier height and ideality factor dependency on identically produced small Au/p-Si Schottky barrier diodes, *J. Semicond.* 31 (2010) 074001.
- [17] A. Elhaji, J.H. Evans-Freeman, M.M. El-Nahass, M.J. Kappers, C.J. Humphries, Electrical characterization and DLTS analysis of a gold/n-type gallium nitride Schottky diode, *Mater. Sci. Semicond. Process.* 17 (2014) 94–99.
- [18] J. Bisquert, *Nanostructured Energy Devices: Equilibrium Concepts and Kinetics*, CRC Press, Boca Raton, Florida, USA, 2014.
- [19] Y. Liu, J.C.W. Yu, P.T. Lai, Investigation of WO<sub>3</sub>/ZnO thin-film heterojunction-based Schottky diodes for H<sub>2</sub> gas sensing, *Int. J. Hydrogen Energy* 39 (2014) 10313–10319.
- [20] S.K. Cheung, N.W. Cheung, Extraction of Schottky diode parameters from forward current-voltage characteristics, *Appl. Phys. Lett.* 49 (1986) 85.
- [21] D.E. Yıldız, Ş. Altındal, H. Kanbur, Gaussian distribution of inhomogeneous barrier height in Al/SiO<sub>2</sub>/p-Si Schottky diodes, *J. Appl. Phys.* 103 (2008) 124502.
- [22] Z. Tekeli, Ş. Altındal, M. Çakmak, S. Özçelik, The behavior of the I–V–T characteristics of inhomogeneous (Ni/Au)–Al<sub>0.3</sub>Ga<sub>0.7</sub>N/AlN/GaN heterostructures at high temperatures, *J. Appl. Phys.* 102 (2007) 054510.
- [23] R.T. Tung, Electron transport at metal-semiconductor interfaces: general theory, *Phys. Rev. B* 45 (1992) 13509.
- [24] R.T. Tung, Comment on “Numerical study of electrical transport in inhomogeneous Schottky diodes”, *J. Appl. Phys.* 88 (2000) 7368–7369.
- [25] A. Gumus, A. Turut, N. Yalcin, Temperature dependent barrier characteristics of CrNiCo alloy Schottky contacts on n-type molecular-beam epitaxy GaAs, *J. Appl. Phys.* 91 (2002) 245–250.